Available online at www.sciencedirect.com
ScienceDirect
Ceramics International 37 (2011) 145–157
CERAMICS INTERNATIONAL
www.elsevier.com/locate/ceramint

# A new potassium-based bioactive glass: Sintering behaviour and possible applications for bioceramic scaffolds

Devis Bellucci, Valeria Cannillo *, Antonella Sola

*Dipartimento di Ingegneria dei Materiali e dell'Ambiente, Università degli Studi di Modena e Reggio Emilia, Via Vignolese 905, 41125 Modena, Italy*

Received 18 June 2010; received in revised form 15 July 2010; accepted 29 July 2010
Available online 21 August 2010

**Abstract**

Providing structural support while maintaining bioactivity is one of the most important goals for bioceramic scaffolds, i.e. artificial templates which guide cells to grow in a 3D pattern, facilitating the formation of functional tissues. In the last few years, 45S5 Bioglass® has been widely investigated as scaffolding material, mainly for its ability to bond to both hard and soft tissues. However, thermal treatments to improve the relatively poor mechanical properties of 45S5 Bioglass® turn it into a glass-ceramic, decreasing its bioactivity. Therefore, the investigation of new materials as candidates for scaffold applications is necessary. Here a novel glass composition, recently obtained by substituting the sodium oxide with potassium oxide in the 45S5 Bioglass® formulation, is employed in a feasibility study as scaffolding material. The new glass, named BioK, has the peculiarity to sinter at a relatively low temperature and shows a reduced tendency to crystallize. In this work, BioK has been employed to realize two types of scaffolds. The obtained samples have been fully characterized from a microstructural point of view and compared to each other. Additionally, their excellent bioactivity has been established by means of *in vitro* tests.


*Keywords:* B. Porosity; D. Glass; D. Glass ceramics; E. Biomedical applications

## 1. Introduction

Until the end of the 1960s, the concept of a material that would not be rejected by living tissues when implanted into the body seemed unimaginable. Biomaterials, in fact, were mainly selected to minimize the formation of fibrous or scar tissue at the interface with host tissues [1,2]. Thanks to the investigations by Hench and co-workers, for the first time the chemical composition of a special family of glasses able to bind to the bone was determined [3,4]. The bioactivity of these glasses is attributed to the formation of a hydroxyapatite (HA) layer on their surface in a biological environment [5,6]. In fact, HA is chemically and structurally very similar to the calcium phosphate mineral present in the human bone tissue, therefore osteoblasts can proliferate on this HA layer and a strong bond can form with the surrounding bone. Among bioactive glasses, the so-called 45S5 Bioglass®, containing 45 wt% $SiO_2$, 24.5 wt% CaO, 24.5 wt% $Na_2O$ and 6 wt% $P_2O_5$, is the most bioactive one, being able to bond both to hard and soft connective tissues [5].

The bioactivity of these materials is usually tested *in vitro*, i.e. by investigating their ability to form a superficial HA layer when soaked in a simulated body fluid (SBF) solution, an acellular solution with inorganic ion concentrations similar to those of the human plasma [7,8]. The *in vitro* HA formation, in fact, is considered as a necessary requirement for an adequate integration of the implant also *in vivo*.

The bioactivity of glasses is deeply influenced by their composition. For example, glasses with a $SiO_2$ content between 52 and 60 wt% can bond to bone, but their bonding rate is very slow. If the $SiO_2$ content further increases, exceeding 60 wt%, glasses do not bond to bone any more and are substantially bioinert. An overview of different bioactive glasses along with their composition and bioactivity degree can be found in Refs. [9,10]. However, it is worth noting that the bioactivity of glasses also depends on their specific surface area. In fact, increasing the glass surface area usually extends the range of bone-bonding compositions to higher $SiO_2$ percentages [4]. This is the case, for example, of fine glass particles used as fillers in the reconstruction of small bone defects. Moreover the enhanced

* Corresponding author. Tel.: +39 059 2056240; fax: +39 059 2056243.
*E-mail address:* valeria@unimore.it (V. Cannillo).

0272-8842/$36.00 
doi:10.1016/j.ceramint.2010.08.020

glass reactivity due to the increased specific surface will be crucial for scaffold technology, as shown in the next paragraphs.

Despite all the biocompatibility tests and toxicology studies performed on bioactive glasses since their discovery, it was only by the mid 1980s that sufficient animal data became available to ensure their clinical safety and efficacy, opening up the possibility to employ them as prosthesis materials. Presently, 45S5 Bioglass® is widely used for orthopedic bone grafting, middle ear implants, dental and maxillofacial applications [11–14].

In the last few years, the use of 45S5 Bioglass® for scaffolding applications has been proposed by several authors, mainly due to its high bioactivity degree [15,16]. Scaffolds are among the key ingredients in bone tissue engineering, being artificial extracellular matrices able to drive and support three-dimensional tissue regeneration. Bone repair by means of tissue engineering protocols is becoming an important and promising field of investigation, since it makes it possible to overcome several shortcomings of conventional approaches such as autografts, i.e. the use of materials coming from the patient body, and allografts, i.e. the use of materials coming from an external donor. Autografts, in fact, are strictly limited by the volume of bone that can be safely obtained and by donor site morbidity. On the other hand, allografts introduce the possibility of immune rejections or pathogen disease transfers [17–19].

Ideal scaffolds should fulfil several criteria [20–22]. First, they should be biocompatible and bioactive. Moreover, they should have an open and interconnected porosity higher than 50–60 vol%, with pore sizes larger than 100 μm in order to satisfy cell size and migration requirements; the fundamental goal, in fact, is to replicate the typical porosity of bone tissue. Many authors have reported that very large pores, with a diameter of some hundred microns, could be extremely effective [23,24]. However also micropores, smaller than 10 μm, are required to promote fluid diffusion. In addition, a rough surface is an ideal texture to foster progenitor cell attachment and adsorption of biological metabolites. Finally, the scaffolds should have adequate mechanical properties matching those of the bone to be repaired, and should bond to it by means of a stable interface.

The use of porous bioactive glasses as scaffolding materials is limited by their intrinsic mechanical weakness and brittleness. Unfortunately, the usual sintering treatments employed to enhance their mechanical properties are performed in a range of temperatures between 900 and 1100 °C, causing the Bioglass® to crystallize into a glass-ceramic [15]. Although this fact does not compromise the formation of a bone–biomaterial bonding, nevertheless the HA formation *in vitro* as well as the bonding process *in vivo* are slowed down by crystallization. Additionally the rate of HA formation decreases when the percentage of crystallization increases [25,26]. For this reason, the mechanisms that turn bioactive glasses into glass-ceramics during thermal treatments and the bioactivity degree of partially crystallized systems are crucial issues. Moreover, it is important to identify new bioactive glass compositions with a reduced tendency to crystallize. These new bioactive glasses can open unexpected and intriguing scenarios for scaffold fabrication.

Recently a novel glass composition, named BioK and obtained by substituting the sodium oxide with potassium oxide in the 45S5 Bioglass®, was formulated [27]. The potassium oxide is expected to reduce the tendency to crystallize of the parent glass [28].

In this work, for the first time the behaviour of BioK powders as a function of the increasing temperature is studied. The identified sintering temperature is significantly lower with respect to the high-temperature cycles usually employed to sinter 45S5 Bioglass® powders [15,29,30]. This fact helps to maintain the amorphous nature of BioK. Moreover, it should be noted that a thermal treatment at lower temperature also results in a cheaper technological protocol.

In a feasibility study, the BioK was used to realize two kinds of bioceramic scaffolds based on powder pressing and sintering. The first type of samples was fabricated by means of the standard polymer burning out method [31], which employs organic particles as pore generating agents in a ceramic matrix. This method combines versatility and low cost. The second type of scaffolds was obtained by employing sodium chloride particles as pore generating agents. This approach was based on the unique thermal behaviour of BioK, which can be sintered at a relatively low temperature. Unlike the burning out method, here the porogens remained unaltered during the entire sintering process, being easily removed by salt leaching at the end of the thermal cycle. The resulting structure is surprisingly compact and highly porous. Finally, the bioactivity of the obtained samples was tested *in vitro* according to the standard protocol developed by Kokubo and co-workers [7,8].

## 2. Materials and methods

### 2.1. BioK fabrication

The BioK composition was inspired by that of the 45S5 Bioglass®, but the sodium oxide was substituted by potassium oxide. The resulting BioK proportions are 46.1 mol% $SiO_2$, 26.9 mol% CaO, 24.4 mol% $K_2O$ (which substituted $Na_2O$), 2.6 mol% $P_2O_5$. A preliminary characterization of this glass can be found elsewhere [27]. BioK was prepared by melting the raw powder materials (commercial reagent-grade $SiO_2$, $CaCO_3$, $K_2CO_3$ and $K_3PO_4{\cdot}H_2O$ by Carlo Erba Reagenti, Italy) in a platinum crucible at 1450 °C for 1 h. The molten glass was then rapidly quenched in cold water to obtain a frit that was subsequently ball-milled and sieved to a final grain size below 70 μm. The final grain size distribution was measured by a laser granulometer (Mastersizer 2000, Malvern Instruments, England); it is reported in Fig. 1.

### 2.2. BioK characterization

The BioK behaviour as a function of the temperature was first investigated by means of an optical dilatometer (Misura

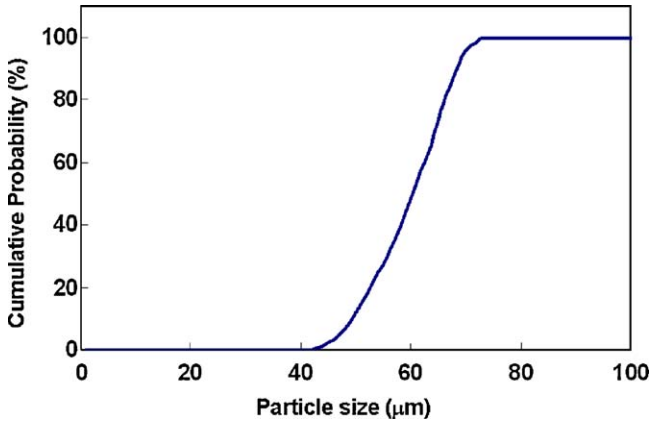


Fig. 1. Particle size distribution of the BioK glass (starting material).

3.32, Expert System Solutions), in order to identify the sintering and the melting temperatures of the glass. The effect of the firing temperature on BioK specimens, obtained by pressing the pure BioK powders at the same conditions used for the scaffolds, was also investigated in a scanning electron microscope, SEM (ESEM Quanta 200, FEI Co., Eindhoven, The Netherlands). The instrument was operated in low-vacuum mode, with a pressure of 0.5 Torr. The chemical analyses were performed by X-ray Energy Dispersion Spectroscopy, EDS (Inca, Oxford Instruments, UK). Moreover, the BioK specimens were also characterized by means of X-ray diffraction (XRD) in order to investigate the crystallinity of the BioK after sintering. The samples were preliminarily ground to obtain a fine powder and then analyzed by means of a PANalytical X'pert PRO diffractometer employing Cu Kα radiation. Data were collected in the angular range 10–70° 2$\theta$, with steps of 0.02° and 5 s/step.

### 2.3. Fabrication of scaffolds via burning out (PolyS scaffolds)

The obtained glass was tested to realize a first type of scaffolds by means of the standard polymer burning out approach [31]. To this aim, 50 vol% of BioK powders were mixed with 50 vol% of polyethylene powders (Goonvean Fibres, UK), a thermally removable organic phase acting as pore generating agent. The following mixture was employed for polyethylene powders: 50 wt% with particle size within 90–150 μm and 50 wt% with particle size within 300–500 μm. This choice was the result of several tests, with the aim to produce samples characterized by the best compromise between porosity and compactness.

The BioK and polyethylene powders were mixed for 30 min in a plastic bottle using a rolls shaker in order to achieve an effective mixing. Subsequently, green bodies were obtained by uniaxial pressing at 140 MPa using propanol as liquid binder. The green bodies were then thermally treated in order to remove the binder and the polyethylene powders while sintering the BioK ones. The thermal treatment was set at a final temperature of 750 °C for 3 h. The heating rate was 10 °C/min.

The acronym PolyS will be used, from now on, to name these scaffolds.

### 2.4. Fabrication of scaffolds via salt leaching (SaltS scaffolds)

In this case BioK powders were mixed with sodium chloride powders sieved to a final grain size below 500 μm. As for PolyS samples, various glass-to-sodium chloride ratios were tested in order to obtain the best compromise between porosity and compactness. The following glass-to-sodium chloride ratios were selected:

- BioK1: 40 vol% of BioK powders and 60 vol% of sodium chloride powders.
- BioK2: 30 vol% of BioK powders and 70 vol% of sodium chloride powders.

The BioK and sodium chloride powders were mixed in a polyethylene bottle using rolls shaker. Then, green bodies were obtained by uniaxially pressing the powders at 140 MPa using acetone as liquid binder. Subsequently, the green bodies were heat-treated in a furnace at 750 °C for 3 h with a heating rate of 10 °C/min. However, while in PolyS samples the porogens were removed during the sintering process – the polyethylene particles are burnt out at a relatively low temperature, about 400 °C, when the glass particles are not yet densified –, in this case the sodium chloride particles did not melt and preserved their original shape during the entire sintering process. Afterwards, the samples were retrieved from the furnace and cooled down to room temperature. The sodium chloride particles were removed from the scaffold by salt leaching. To this aim, the samples were briefly immersed in distilled water at 80 °C. The water was agitated by magnetic stirring and frequently replaced. Finally, the scaffolds were dried overnight in a furnace at 110 °C.

The acronym SaltS will be used, from now on, to name these scaffolds. In particular, SaltS_1 and SaltS_2 will indicate the samples fabricated employing the BioK1 and BioK2 compositions, respectively.

### 2.5. Scaffolds characterization and assessment of bioactivity in simulated body fluid

The porosity of the scaffolds was calculated by

$$P_{\%} = \left(1 - \frac{W_f}{W_0}\right) \times 100$$

where $P_{\%}$ is the total pore content (vol%), $W_f$ is the measured weight of the scaffold and $W_0$ is the theoretical one, obtained by multiplying the scaffold volume by the BioK density. The volume of the scaffolds was easily measured, since the pressed samples were shaped in form of disks (4.0 cm of diameter, 0.7 cm of thickness for PolyS and 0.8 cm for SaltS, respectively). The density $\rho = 2.65$ g/cm$^3$ of the glass was measured by means of a pycnometer test (Micromeritics AccuPyc 1330,

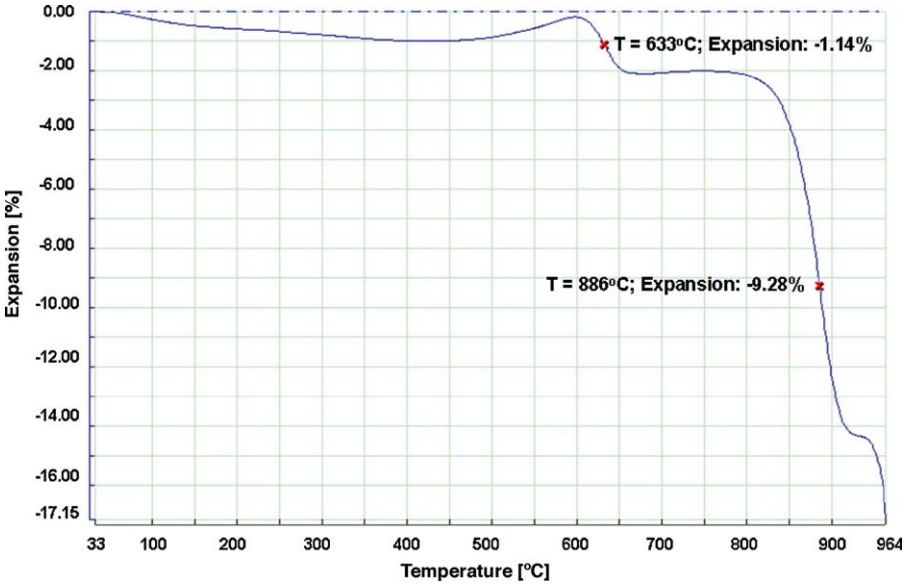


Fig. 2. Optical dilatometer analysis of the BioK powders.

Georgia, USA). For each type of scaffold, five specimens were evaluated. Optical microscope images were also considered and analyzed with the aim to validate the porosity values. In particular, for each kind of scaffold, at least five images were acquired with an optical microscope equipped with a 10× objective. The area occupied by the pores was quantified by means of image analysis (UTHSCSA Image Tool).

A complete morphological characterization was carried out on the scaffolds by means of a SEM equipped with EDS. The scaffolds were also characterized through X-ray diffraction analysis. The SEM and XRD analysis were performed under the same conditions as described in Section 2.2.

The scaffolds bioactivity was evaluated *in vitro* using the standard protocol developed by Kokubo and co-workers [7,8]. In order to reproduce *in vitro* the formation of HA in scaffolds, PolyS and SaltS samples were immersed in flasks containing 20 ml of a simulated body fluid. The flasks were placed inside an incubator at a controlled temperature of 37 °C. The SBF was refreshed every 2 days. After given times of 3, 7 and 14 days the samples were extracted, rinsed with deionized water and then left to dry at ambient temperature. The evaluation of the amount and morphology of the precipitated HA on the samples surface was carried out by SEM (equipped with EDS) and XRD analysis.

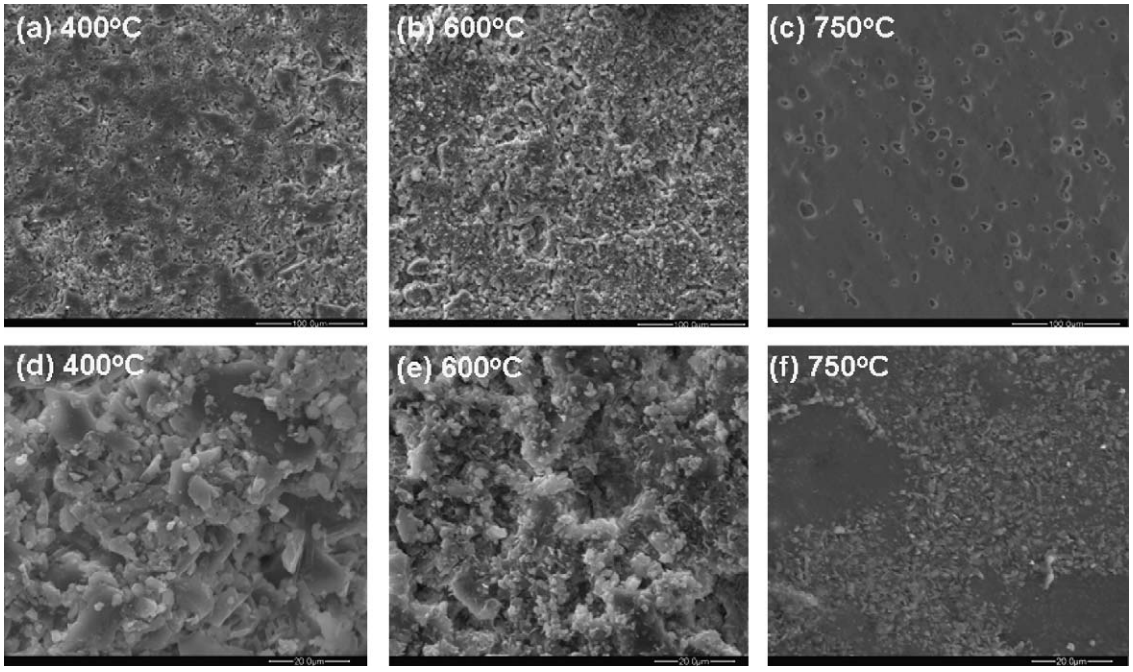


Fig. 3. Micrographs of a BioK specimen, obtained by powders pressing, as a function of the increasing temperature.

## 3. Results and discussion

### 3.1. BioK characterization

Fig. 2 shows the results of the optical dilatometer analysis carried out on the BioK powders, which gives useful indications about the sample sintering kinetics, since sintering is usually accompanied by high specimen shrinkages. It is possible to observe a two-step sintering process: the first one between 600 and 650 °C (maximum shrinkage rate at 633 °C) and the second one between 800 and 900 °C (maximum shrinkage rate at 886 °C). Then, a third step begins at high temperature, about 950 °C, where the sample starts to soften and finally melts. However, as reported in the next paragraphs, preliminary tests carried out at 600 and 650 °C showed that these temperatures were not high enough to sinter the glass particles in samples containing also pore generating agents, such as PolyS and SaltS scaffolds. In particular, in PolyS samples, the polyethylene powders are thermally removed at about 400 °C, when the glass struts are not well densified yet. In this case, the struts themselves may collapse and clog the pores, resulting in a poor interconnected porosity. Finally, the gas release caused by the polyethylene burning out may further increase this effect. The optimal heat treatment was identified to be 750 °C for 3 h. On the one hand, in fact, such a temperature ensures the complete vaporization of the organic porogens in PolyS samples with no residual contamination, on the other hand it is not high enough to melt the sodium chloride particles in SaltS samples. In this way it was possible to fabricate PolyS and SaltS samples at the same temperature, making it easier to compare their microstructure.

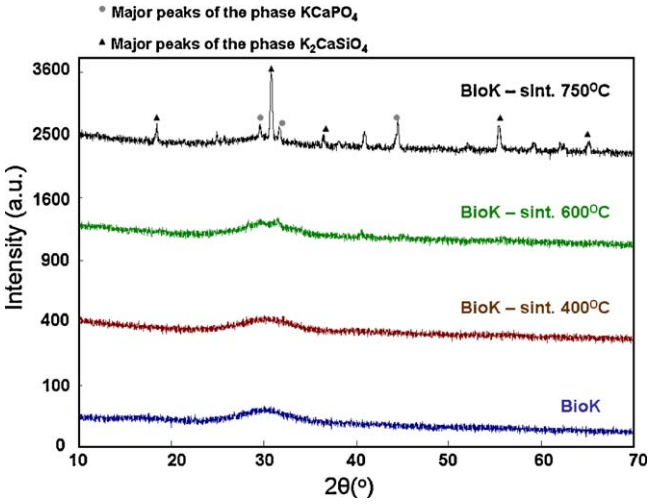


Fig. 4. XRD spectra of the BioK starting powders and of a BioK specimen treated at different temperatures and ground into powder.

The effect of the firing temperature on the BioK alone, with no porogen addition, can be appreciated observing Fig. 3. In fact, Fig. 3 reports some representative micrographs of BioK specimens obtained by pressing the pure BioK powders at the same conditions used for the scaffolds and firing them at various temperatures. Fig. 3 shows the final microstructure as a

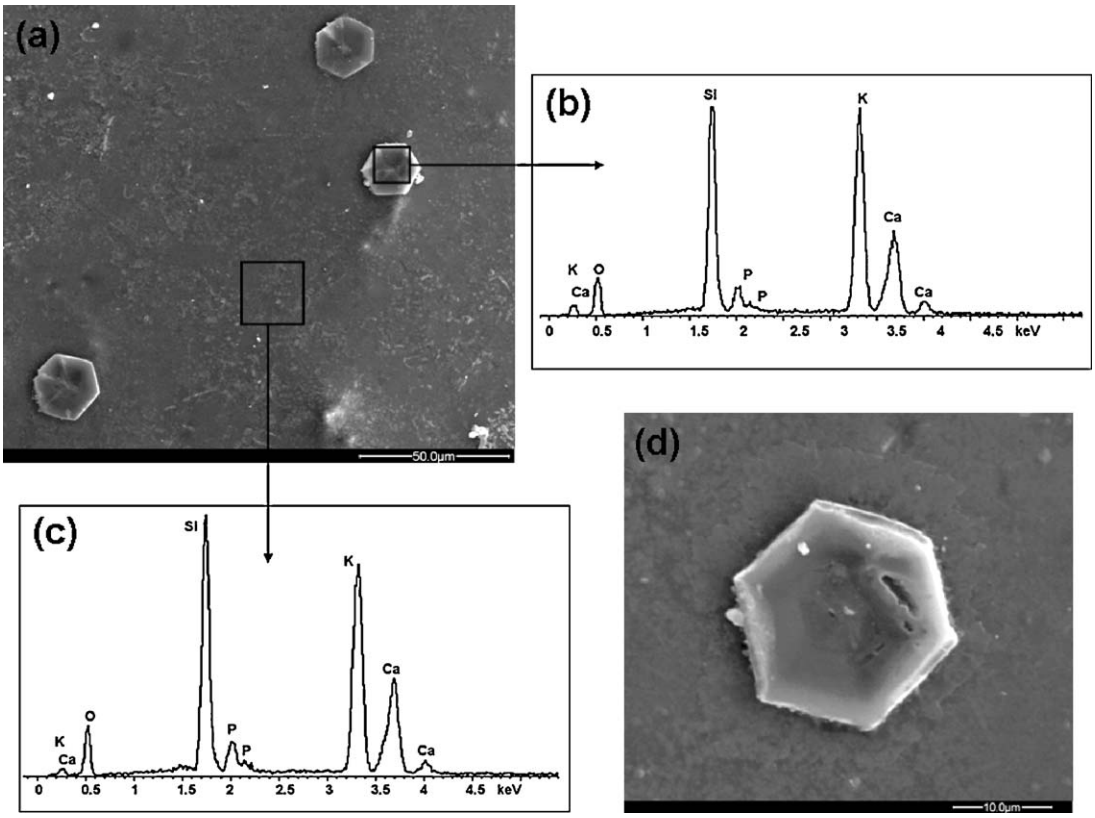


Fig. 5. Micrographs and EDS analysis of a BioK specimen, obtained by powders pressing and subsequently sintering at 750 °C. Hexagonal crystals on the surface of the sintered material can be observed (a, d).

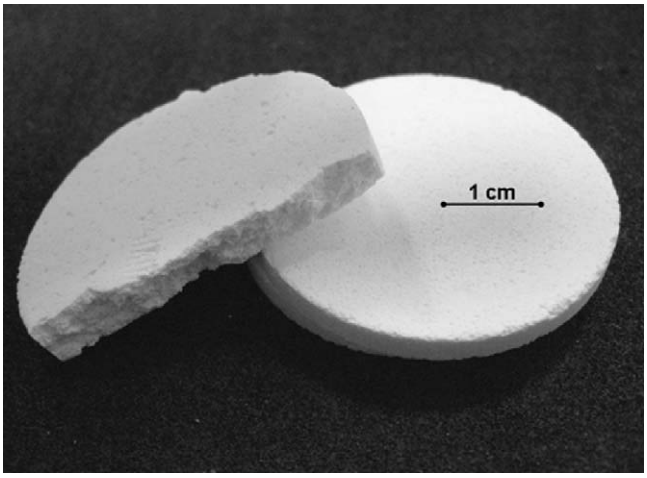


Fig. 6. Photograph of SaltS_1 samples.

function of the increasing temperature at low (a, b, c) and high (d, e, f) magnification. The specimen in Fig. 3(a) and (d) shows that at 400 °C the system is poorly densified: there are large voids on the surface texture and it is possible to identify the starting glass particles. The densification, which accompanies the sintering process, is observable in Fig. 3(b) and (e). In particular, at 600 °C the optical dilatometer analysis reports the beginning of the specimen shrinkage. The particles start to adhere to one other and locally some pores increase their size while the system rearranges. At 750 °C, as shown in Fig. 3(c) and (f), the system is well densified.

Fig. 4 shows the XRD analysis performed on the BioK starting powders and on the BioK abovementioned specimens ground into a powder. Also in this case, the analysis was performed on samples treated at 400, 600 and 750 °C. Up to 600 °C, the patterns indicate that the system remains almost amorphous. At 600 °C a slight devitrification appears, as witnessed by some small peaks in the corresponding XRD pattern. The peaks observed at 750 °C reveal the presence of two main crystalline phases, identified as $K_2CaSiO_4$ and $KCaPO_4$. However, also in this case the broad halo, typical of glasses, is still present, confirming the limited tendency to crystallize of the BioK. It should be noted that improving the mechanical properties of the glass by means of a complete sintering, while retaining its amorphous nature, is crucial in order to preserve the material and the resulting scaffold bioactivity. From this point of view, in the last few years many works in the literature have discussed the effect of the temperature on the bioactivity of the widely used 45S5 Bioglass®, and the debate is still open [25,32,33,37]. Many authors, in fact, have observed a complete crystallization of 45S5 Bioglass® at the temperatures usually employed to fabricate scaffolds, by both the burning out method and the foam replication technique [15].

Micrographs and EDS analysis of the considered BioK specimens are reported in Fig. 5. Hexagonal crystals on the surface of the sintered material can be occasionally observed (Fig. 5(a) and (d)). The EDS analysis (Fig. 5(b) and (c)) shows that the chemical composition of the hexagonal crystals slightly differs in potassium content from the environment one.

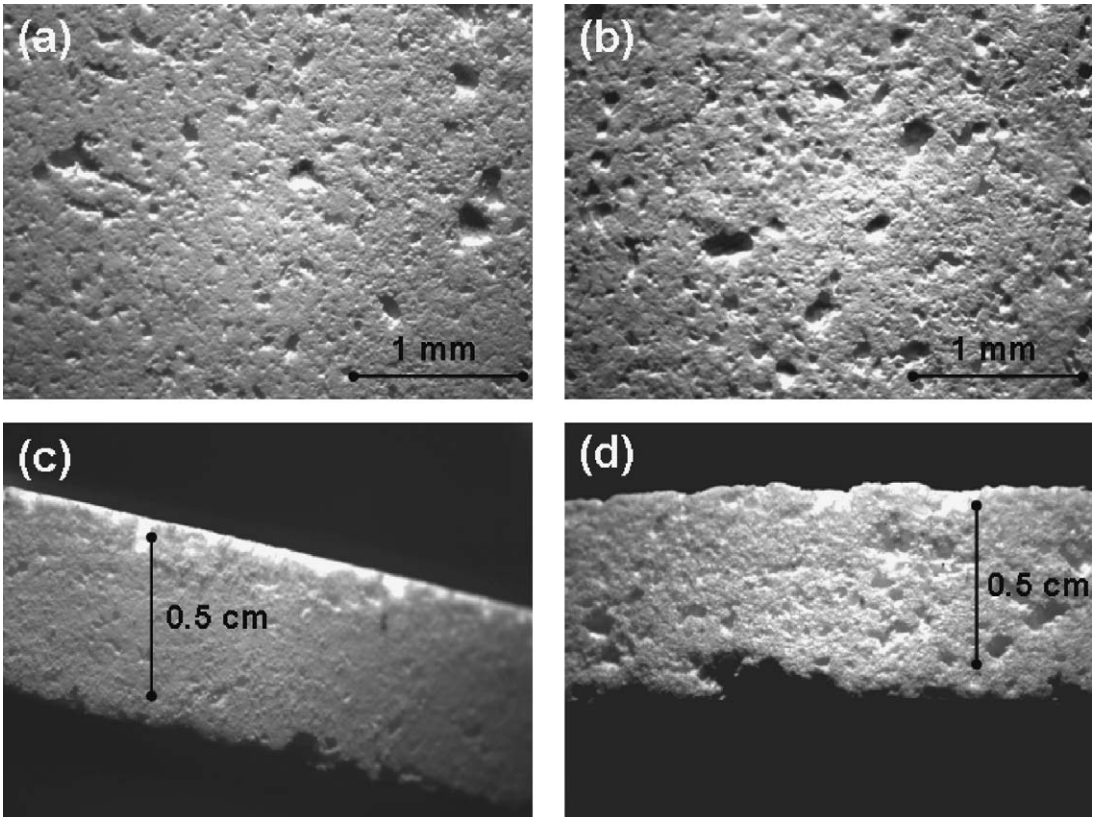


Fig. 7. Photograph of SaltS_1 (a, c) and SaltS_2 (b, d) samples surface.

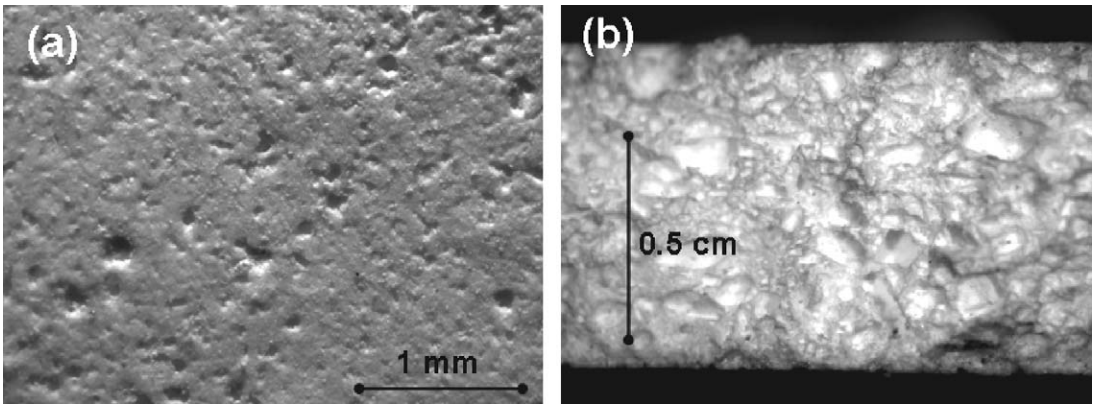


Fig. 8. Photograph of the PolyS sample surface.

However, this analysis is not trivial, since the crystals thickness is very small compared to the typical volume analyzed by the EDS probe.

### 3.2. Scaffold characterization

PolyS and SaltS samples are quite similar from a macroscopic point of view. A photograph of a SaltS_1 sample is reported in Fig. 6. Fig. 7 shows SaltS_1 and SaltS_2 samples with details of the external surface perpendicular (Fig. 7(a) and (b)) and parallel (Fig. 7(c) and (d)) to the pressing direction. It is possible to note the presence of a large amount of pores in both samples. However SaltS_2 samples, prepared using a lower amount of glass, seem to possess a larger porosity compared to SaltS_1 ones. An example of a PolyS sample surface is reported in Fig. 8.

Micrographs of the internal structure of SaltS_1 and the PolyS at different magnifications are reported in Figs. 9 and 10, respectively. Independently of the fabrication process, the

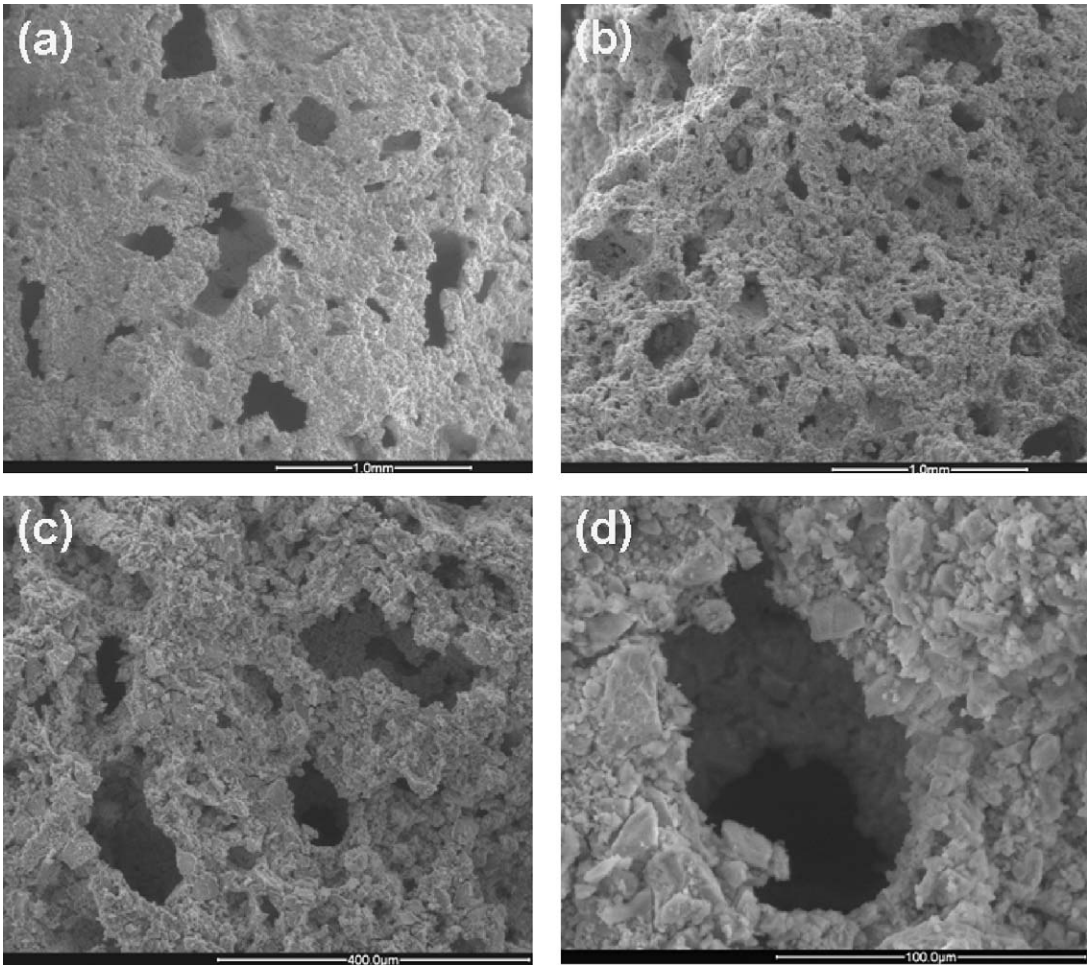


Fig. 9. Micrographs of the SaltS_1 internal structure at different magnification degrees.

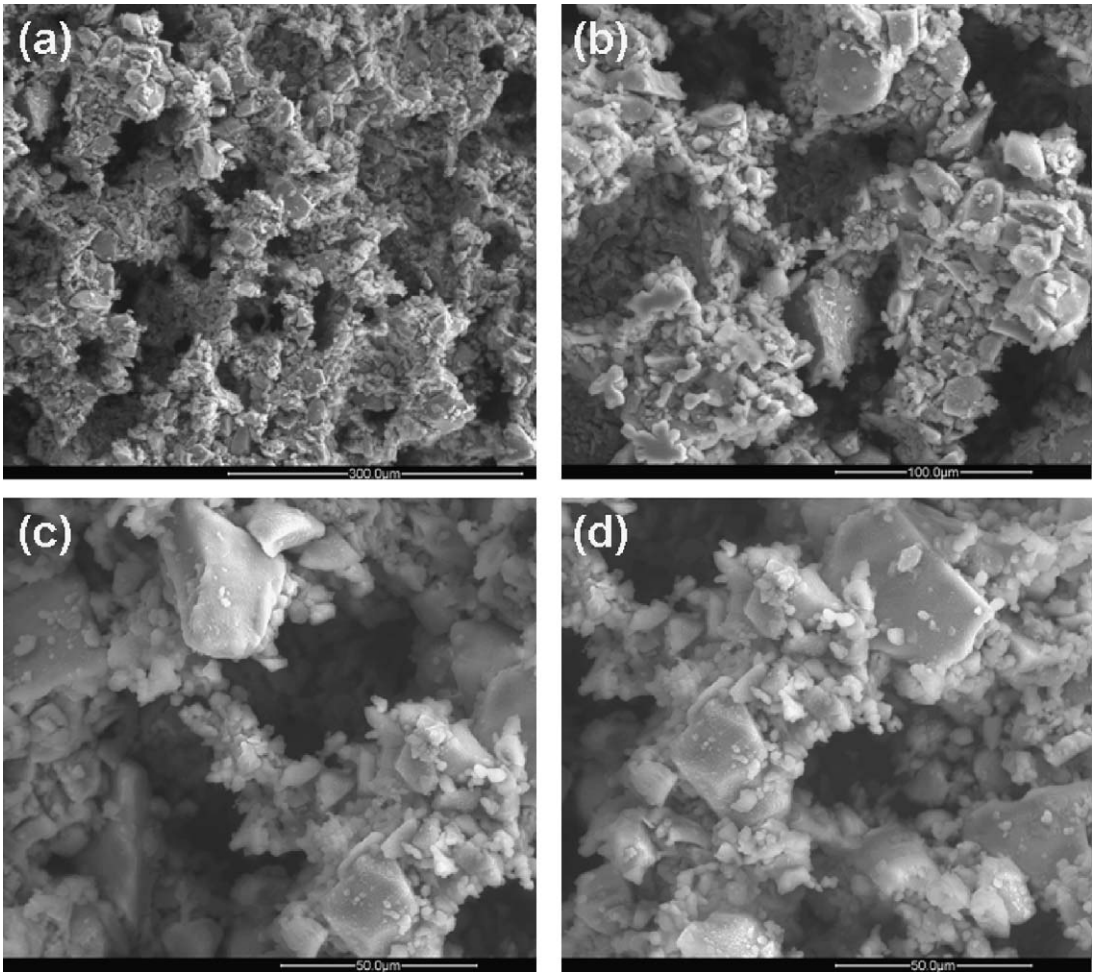


Fig. 10. Micrographs of the PolyS internal structure at different magnification degrees.

samples are characterized by an open macroporosity in the range of a few hundreds of μm. The average pore size lies within a critical range, i.e. 100–200 μm, which satisfies the requirements to allow ingrowth of osteoblast cells inside the scaffold [20,21]. Additionally, it is possible to note a widespread microporosity on the struts between the pores, which plays a fundamental role in ensuring the adequate angiogenesis together with the diffusion of fluids and nutrients [34]. A good sintering level was achieved, although the thermal treatment was performed at a relatively low temperature. Finally, the rough texture which covers the scaffold surface is a key factor to foster the attachment of proteins and bone proliferation cells [35], as already mentioned in the introduction. The average porosity was about 60 (±3) vol% for PolyS

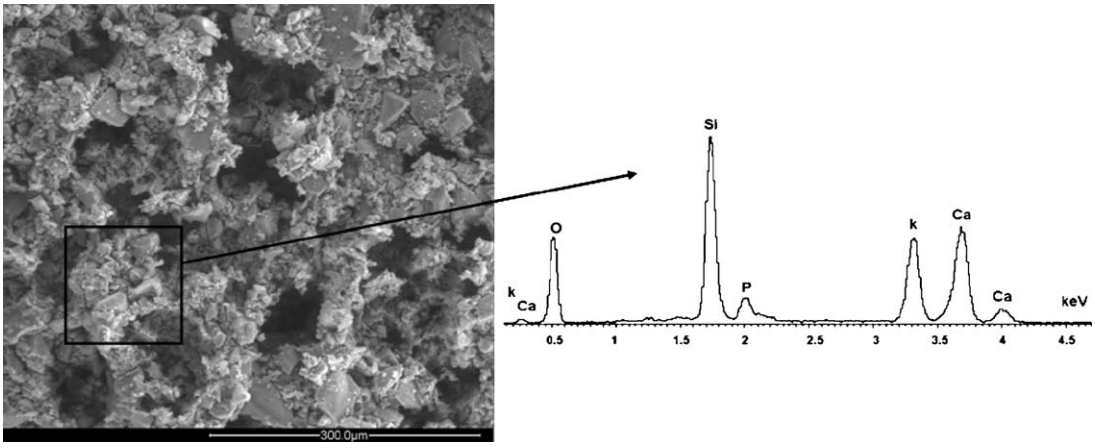


Fig. 11. EDS analysis of the whole area reported, which refers to the PolyS internal structure.

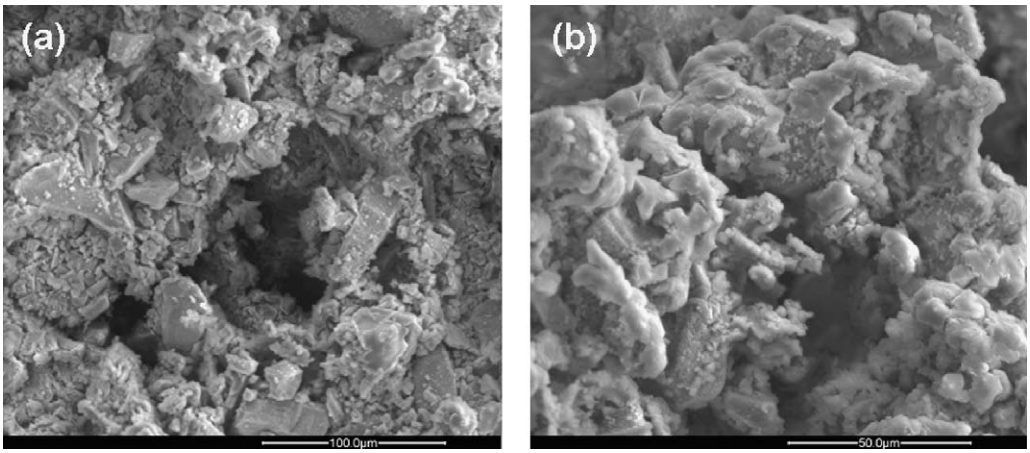


Fig. 12. The PolyS surface after immersion in simulated body fluid for 3 days.

samples. This value is satisfactory, in particular taking into account the values commonly reported in literature for scaffolds based on a burning out approach [31]. However the novel NaCl-based protocol, employed to fabricate SaltS samples, is a substantial improvement compared to the classical burning out approach. In fact, it makes it possible to achieve the same porosity level which is usually produced by means of more sophisticated (and complex) techniques [15]. The average porosity, in fact, is about 70 (±2) vol% and 75 (±2) vol% for SaltS_1 and SaltS_2, respectively. The calculated porosity values were also confirmed by image analysis both for SaltS and PolyS scaffolds. However, it should be noted that the values calculated by means of this technique presumably approximate the real porosity: on the one hand, indeed, relatively low magnification (10×) images are required to appreciate large pores, but small pores cannot be detected clearly; on the other hand, the calculated values are based on 2D images, while the real porosity is intrinsically 3-dimensional and highly interconnected.

Moreover, in spite of their porosity, the SaltS samples look surprisingly compact and manageable with no damage. Unlike PolyS scaffolds, in fact, where the removal of the porogens occurred when the glass had not been sintered yet, in SaltS

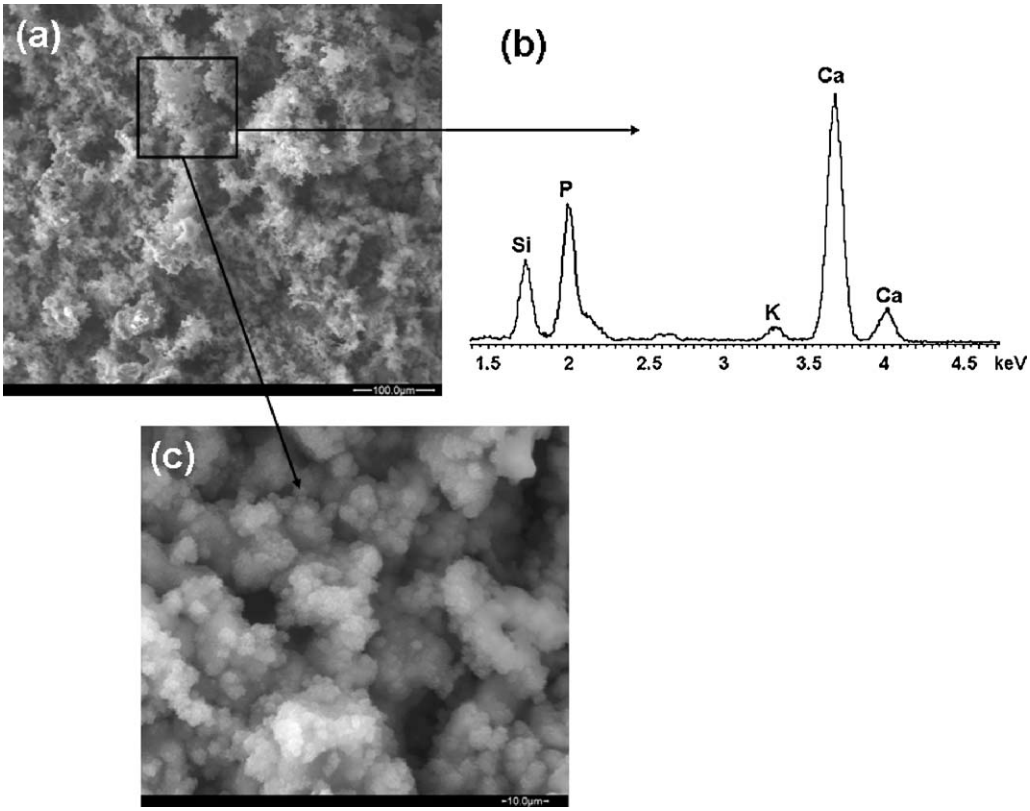


Fig. 13. Hydroxyapatite formed on the surface of PolyS scaffolds after immersion in simulated body fluid for 7 days. (c) Detail and (b) EDS results of the analysis carried out on the whole area reported in (a).

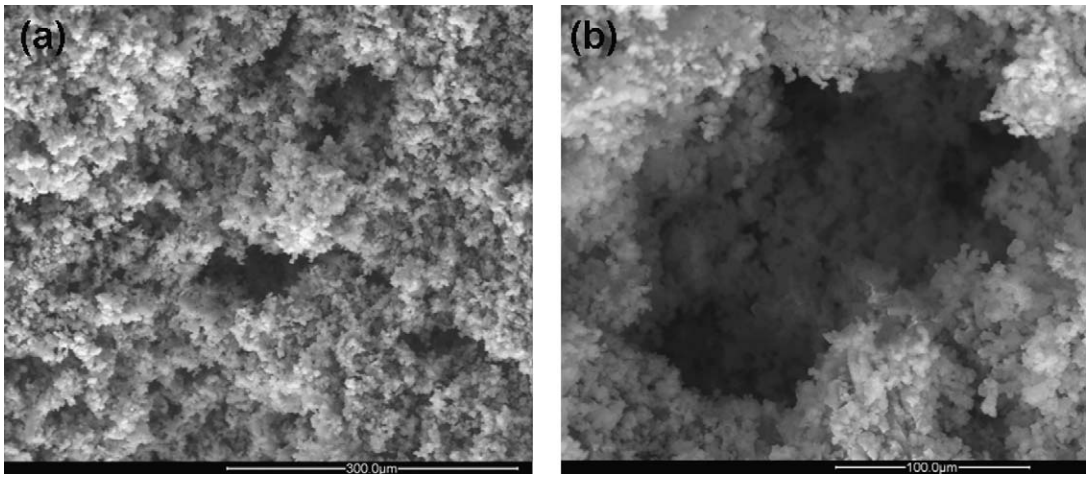


Fig. 14. Hydroxyapatite formed on the surface of PolyS scaffolds after immersion in simulated body fluid for 14 days.

scaffolds the thermal treatment did not decompose the pore generating agents, i.e. sodium chloride particles, which remained unchanged in the glass matrix during the whole sintering process. In this way, the porogens ensured a proper support to the pore walls during sintering and maintained their shape until an adequate densification of the glass struts was achieved. Therefore it was possible to avoid any collapse and obstruction of the pores.

In addition, the PolyS microstructure appears to be more heterogeneous compared to the SaltS one; this fact is probably due to the evaporation of the organic phase. It should be noted that the novel fabrication protocol based on the salt leaching, which is easy to realize and, at the same time, represents a substantial step forward in respect to the burning out method, was made possible by the intriguing properties of the new BioK composition. Although an evaluation of the mechanical strength of the scaffolds goes beyond the scope of this work, the SaltS scaffolds look rather promising compared to PolyS ones.

Fig. 11 shows the EDS analysis performed on the PolyS internal structure. The chemical species that characterize the system, together with their relative amount, can be observed. The SaltS EDS pattern is analogous to the PolyS one, therefore

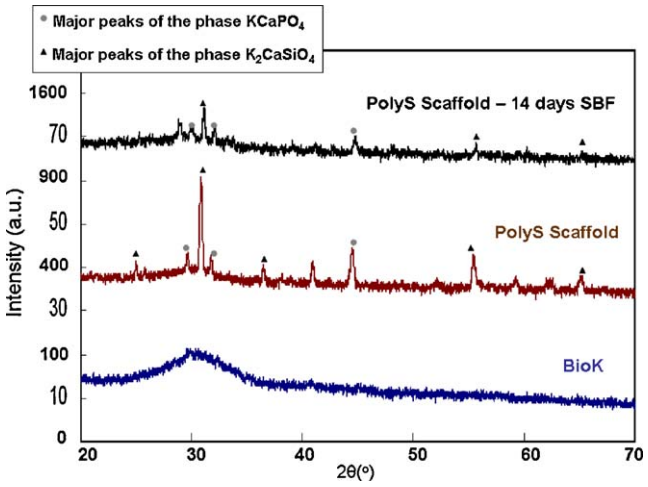


Fig. 15. XRD analysis of a PolyS sample before and after soaking in SBF for 14 days.

it is not reported. It is important to note that, as regards the *in vitro* HA precipitation, the potassium ion, which is clearly visible in the BioK composition also after thermal treatment, plays the same role as the sodium ion in 45S5 Bioglass®. According to the model proposed by Hench [5,35–37], in fact, the HA precipitation process, which prepares the ground to the cellular adhesion, begins with ion leaching: the glass starts its dissolution by exchanging $K^+$ (or $Na^+$) cations with $H^+$ or $H_3O^+$ ions from the physiological solution. This first step, which determines an increase of the interfacial pH, is followed by the breaking of Si–O–Si bonds in the glass network and the subsequent formation of silanol groups (Si–OH) at the glass/solution interface. The polycondensation of neighbouring silanol groups results in a silica gel layer on the glass surface, depleted in $K^+$ ions. The –OH functional groups act as effective nucleation sites for apatite precipitation and crystallization [38,39]. Once the HA nuclei are formed, they would spontaneously grow thanks to the migration of calcium and phosphate groups from the physiological solution. The results of the *in vitro* tests performed on the scaffolds, which will be reported in the next sections, can be interpreted following the abovementioned model.

Fig. 12 shows the PolyS surface after immersion in simulated body fluid for 3 days. A silica gel covers the surface (Fig. 12(b)) that started its dissolution process. It is possible to note some white spherical agglomerates on the surface, which can be identified as the first HA nuclei.

The HA formed on PolyS samples after 7 days in SBF is appreciable in Fig. 13. In this case, the sample surface is completely covered by globular precipitates with the typical HA morphology. Some considerations may be made observing the EDS spectrum depicted in Fig. 13(b), which refers to the whole area reported in Fig. 13(a):

- After immersion in SBF, the potassium content of the sample is strongly reduced compared to the spectra reported in Fig. 11. This phenomenon, due to the ion leaching, is accompanied by a SBF supersaturation with respect to HA, through pH increase, and marks the beginning of the crystalline network breakdown.

- The detected intensity of the Silicon peak decreases due to the HA layer above it.
- The EDS analysis shows the presence of Ca and P in proportion similar to that in HA, since the Ca/P ratio is about 1.8 while in the stoichiometric HA it is 1.67 [40].

Fig. 14 shows the PolyS surface after 14 days in SBF. The scaffold is completely covered by HA. HA covers also the internal pore surface (Fig. 14(b)). Many struts have been completely dissolved and it is difficult to identify the original pore network. Apart from local fluctuations, the Ca/P ratio in the globular precipitates approaches 1.67. The pH value reached a steady value between 7.5 and 8.

The XRD analysis of a PolyS sample before and after soaking in SBF for 14 days is reported in Fig. 15. The diffraction pattern of the scaffold was obtained after milling. It

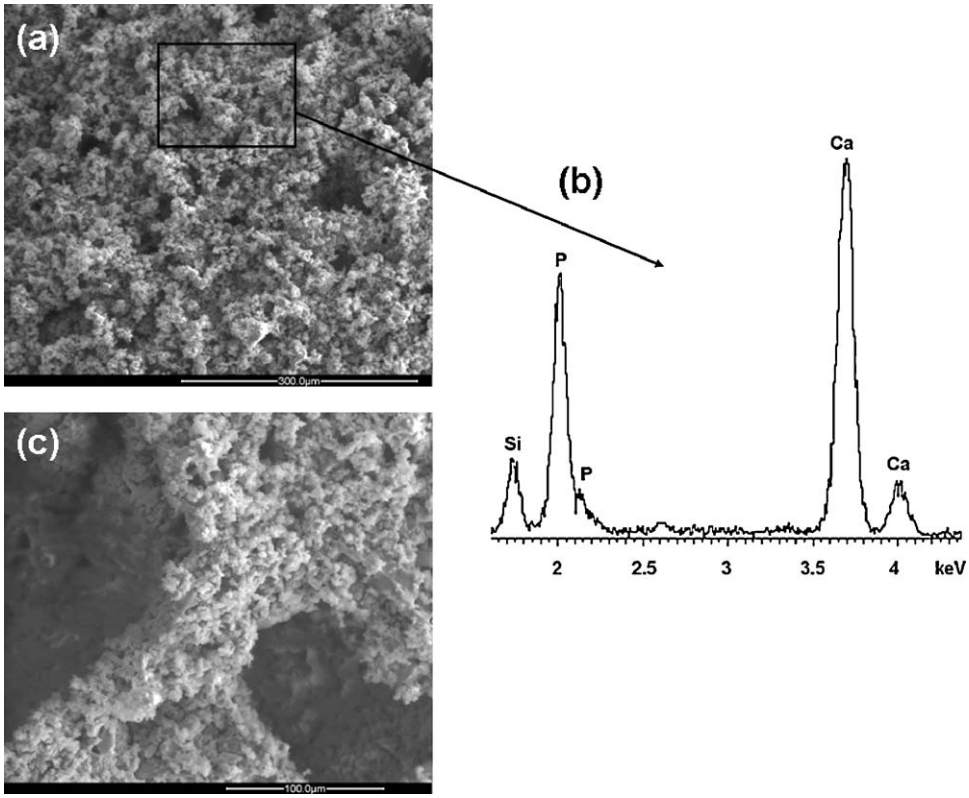


Fig. 16. The SaltS_2 surface after immersion in simulated body fluid for 3 days. (b) EDS results of the analysis carried out on the whole area reported in (a).

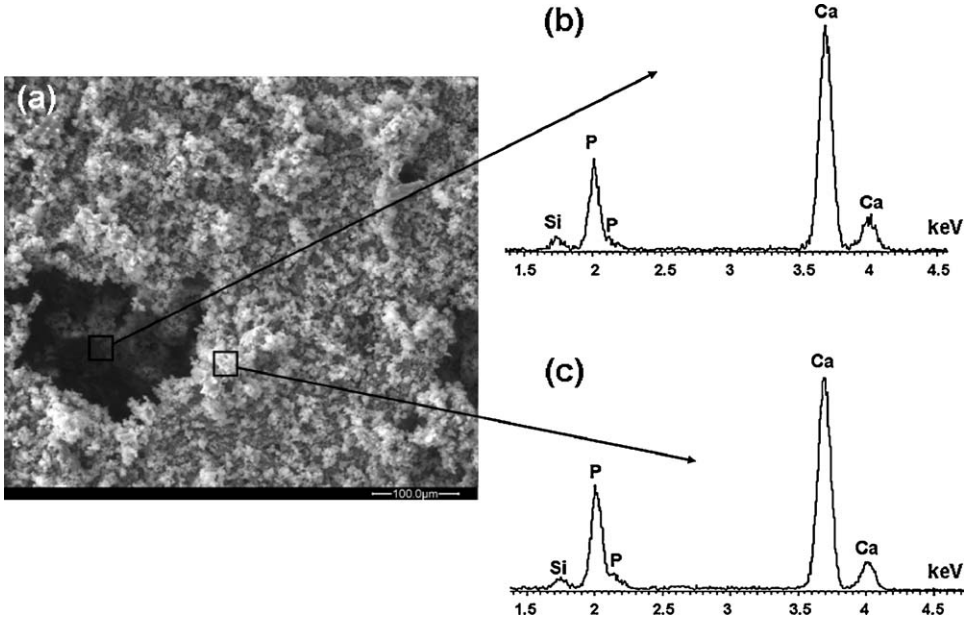


Fig. 17. The SaltS_2 surface after immersion in simulated body fluid for 7 days. (b, c) EDS results of the analysis carried out on the whole areas reported in (a).

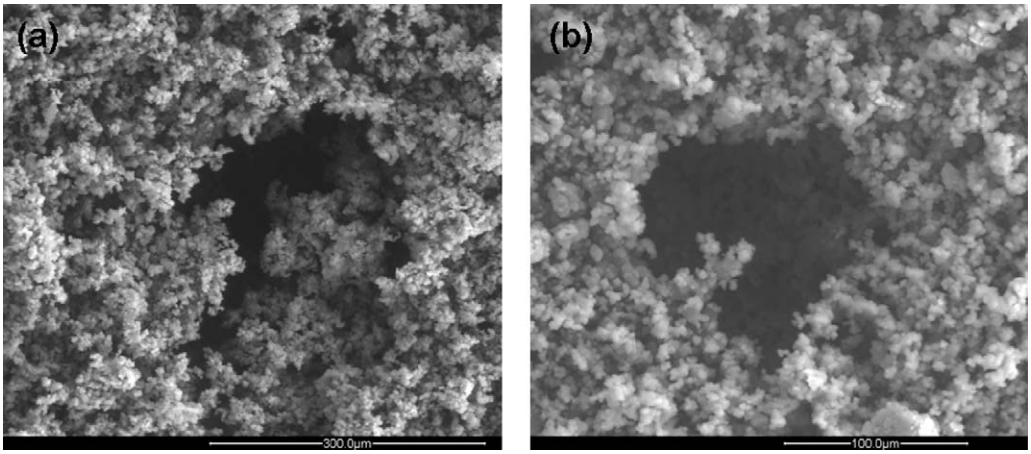


Fig. 18. The SaltS_2 surface after immersion in simulated body fluid for 14 days.

is possible to observe the dissolution of the main crystalline phases. Unfortunately, the peaks of the crystalline phases still present after soaking and the peaks of HA overlap, therefore it was not possible to identify them in the XRD spectra. On the basis of these considerations, a bioactive behaviour of the BioK PolyS samples may be expected.

A similar analysis can be carried out on the SaltS samples. Fig. 16 depicts the SaltS_2 surface after immersion in simulated body fluid for 3 days, together with the results of the EDS analysis. In this case, just after 3 days the surface is completely covered by a HA layer. Additionally, the potassium content of the sample surface approaches to zero, therefore the scaffold surface is almost depleted in $K^+$. For these reasons, SaltS_2 samples seem to be more bioactive compared to PolyS ones. However, this fact can probably be attributed to the SaltS_2 higher porosity degree, which is accompanied by a higher specific surface. The EDS analysis reported in Fig. 17 shows that no differences can be noted between the chemical compositions of the HA precipitate outside and inside a pore. The HA layer, therefore, evenly covers the whole scaffold structure. The Ca/P ratio in the globular precipitates is about 1.7. Also in this case the pH value reached a steady value between 7.5 and 8. Finally, the SaltS_2 surface after 14 days in SBF is reported in Fig. 18. The samples look rather similar to the PolyS ones after the same soaking time, i.e. when also in the latter the dissolution process was advanced. The XRD analysis of the SaltS samples is very similar to the PolyS one, therefore it is not reported. SaltS_1 samples showed an analogous behaviour with respect to SaltS_2 samples, since their porosity degree was almost the same (70 and 75 vol%, respectively).

## 4. Conclusion and perspectives

A new glass composition, recently obtained by substituting the sodium oxide with potassium oxide in the 45S5 Bioglass® formulation, was employed in a feasibility study to produce scaffolds for bone tissue repair. The first part of the work was devoted to a full characterization of the new glass composition, named BioK, in order to investigate its behaviour as a function of the temperature. From this point of view, BioK presents several advantages compared to the widely used 45S5 Bioglass®. In particular it can be treated at a relatively low temperature and it is characterized by a reduced tendency to crystallize. This fact is crucial to preserve the material bioactivity.

In the second part of the work, the new glass was employed to realize two types of scaffolds based on powder pressing and sintering: PolyS scaffolds, used as reference samples, were realized by the standard burning out method, while SaltS scaffolds were fabricated employing a novel protocol recently developed, based on salt leaching. It should be noted that it was possible to obtain SaltS scaffolds mainly thanks to the BioK peculiarity to be sintered at a relatively low temperature. SaltS scaffolds are easy to realize and manageable, in spite of their high porosity, comparable to that obtainable by means of more sophisticated methods. The samples were characterized from a microstructural point of view, while their bioactivity was tested *in vitro* giving excellent results.

In conclusion, the novel BioK glass resulted to be an interesting material for scaffolding applications. Further studies on BioK-derived scaffolds for bone tissue repair are under investigations. In particular, it will be interesting to test *in vivo* the realized samples in a biological reactor. These studies will be the subject of future works.

## References

[1] L.L. Hench, J. Wilson, Surface-active biomaterials, Science 226 (1984) 630–636.
[2] L.L. Hench, Biomaterials: a forecast for the future, Biomaterials 19 (1998) 1419–1423.
[3] K.H. Karlsson, L. Hupa, Thirty-five years of guided tissue engineering, J. Non-Cryst. Solids 354 (2008) 717–721.
[4] L.L. Hench, The story of Bioglass®, J. Mater. Sci.: Mater. Med. 17 (2006) 967–978.
[5] L.L. Hench, Bioceramics, from concept to clinic, J. Am. Ceram. Soc. 74 (7) (1991) 1487–1510.
[6] L.L. Hench, G.P. LaTorre, The reaction kinetics of bioactive ceramics. Part IV. Effect of glass and solution composition, in: Yamamuro, Kokubo, Nakamura (Eds.), Bioceramics, vol. 5, Kobunshi Kankokai Press, 1993, pp. 67–74.
[7] T. Kokubo, H. Takadama, How useful is SBF in predicting *in vivo* bone bioactivity? Biomaterials 27 (2006) 2907–2915.
[8] T. Kokubo, H. Kushitani, S. Sakka, T. Kitsugi, T. Yamamuro, Solutions able to reproduce in vivo surface-structure changes in bioactive glass-ceramic A-W, J. Biomed. Mater. Res. 24 (2004) 721–734.

[9] W. Cao, L.L. Hench, Bioactive materials, Ceram. Int. 22 (1996) 493–507.
[10] M.W.G. Lockyer, D. Holland, R. Dupree, NMR investigation of the structure of some bioactive and related glasses, J. Non-Cryst. Solids 188 (1995) 207–219.
[11] M. Vollenweider, T.J. Brunner, S. Knecht, R.N. Grass, M. Zehnder, T. Imfeld, W.J. Stark, Remineralization of human dentin using ultrafine bioactive glass particles, Acta Biomater. 3 (2007) 936–943.
[12] C.A. Shapoff, D.C. Alexander, A.E. Clark, Clinical use of a bioactive glass particulate in the treatment of human osseous defects, Compend. Contin. Educ. Dent. 18 (1997) 352–358.
[13] E. Douek, Otologic applications of Bioglass® implants, in: W. Bonfield, G.W. Hastings, K.E. Tanner (Eds.), Bioceramics, vol. 4, Butterworth Heinemann, Oxford, 1991.
[14] H.R. Stanley, M.B. Hall, A.E. Clark, C.J. King, L.L. Hench, J.J. Berte, Using 45S5 Bioglass® cones as endosseous ridge maintenance implants to prevent alveolar ridge resorption: a 5-year evaluation, Int. J. Oral Maxillofac. Implants 12 (1997) 95.
[15] Q.Z. Chen, I.D. Thompson, A.R. Boccaccini, 45S5 Bioglass®-derived glass–ceramic scaffolds for bone tissue engineering, Biomaterials 27 (2006) 2414–2425.
[16] D. Bellucci, V. Cannillo, A. Sola, Shell Scaffolds: a new approach towards high strength bioceramic scaffolds for bone regeneration, Mater. Lett. 64 (2010) 203–206.
[17] I. Asahina, I. Seto, M. Oda, E. Marukawa, A.M. Imranul, S. Enomoto, Bone Engineering, 1st edition, Em squared, Toronto, 1999.
[18] J.A. Goulet, L.E. Senunas, G.L. DeSilva, M.L. Greenfeild, Autogenous iliac crest bone graft. complications and functional assessment, Clin. Orthop. Relat. Res. 339 (1989) 76–81.
[19] E.M. Younger, M.W. Chapman, Morbidity at bone graft donor sites, J. Orthop. Trauma. 3 (1989) 192–195.
[20] K. Rezwan, Q.Z. Chen, J.J. Blaker, A.R. Boccaccini, Biodegradable and bioactive porous polymer/inorganic composite scaffolds for bone tissue engineering, Biomaterials 27 (2006) 3413–3431.
[21] V. Karageorgiou, D. Kaplan, Porosity of 3D biomaterial scaffolds and osteogenesis, Biomaterials 26 (2005) 5474–5491.
[22] J.R. Jones, L.L Hench, Regeneration of trabecular bone using porous ceramics, Curr. Opin. Solid State Mater. Sci. 7 (2003) 301–307.
[23] O. Gautier, J.M. Bouler, E. Aguado, P. Pilet, G. Daculsi, Macroporous biphasic calcium phosphate ceramics: influence of macropore diameter and macroporosity percentage on bone ingrowth, Biomaterials 19 (1998) 133–139.
[24] M.C. von Doernberg, et al., In vivo behavior of calcium phosphate scaffolds with four different pore sizes, Biomaterials 27 (2006) 5186–5198.
[25] O.P. Filho, G.P. LaTorre, L.L. Hench, Effect of crystallization on apatite-layer formation of bioactive glass 45S5, J. Biomed. Mater. Res. 30 (1996) 509–514.
[26] O. Peitl, E.D. Canotto, L.L. Hench, Highly bioactive $P_2O_5$–$Na_2O$–CaO–$SiO_2$ glass-ceramics, J. Non-Cryst. Solids 292 (2001) 115–126.
[27] V. Cannillo, A. Sola, Potassium-based composition for a bioactive glass, Ceram. Int. 35 (2009) 3389–3393.
[28] H. Arstila, L. Hupa, K.H. Karlsson, M. Hupa, Influence of heat treatment on crystallization of bioactive glasses, J. Non-Cryst. Solids 354 (2008) 722–728.
[29] J. Qian, Y. Kang, Z. Wei, W. Zhang, Fabrication and characterization of biomorphic 45S5 bioglass scaffold from sugarcane, Mater. Sci. Eng., C 29 (2009) 1361–1364.
[30] O. Bretcanu, X. Chatzistavrou, K. Paraskevopoulos, R. Conradt, I. Thompson, A.R. Boccaccini, Sintering and crystallisation of 45S5 Bioglass® powder, J. Eur. Ceram. Soc. 29 (2009) 3299–3306.
[31] C. Vitale Brovarone, E. Verné, P. Appendino, Macroporous bioactive glass-ceramics scaffolds for tissue engineering, J. Mater. Sci.: Mater. Med. 17 (2006) 1069–1078.
[32] L. Lefebvre, J. Chevalier, L. Gremillard, R. Zenati, G. Thollet, D. Bernache-Assolant, A. Govin, Structural transformations of bioactive glass 45S5 with thermal treatments, Acta Mater. 55 (2007) 3305–3313.
[33] L. Lefebvre, L. Gremillard, J. Chevalier, R. Zenati, D. Bernache-Assolant, Sintering behaviour of 45S5 bioactive glass, Acta Biomater. 4 (2008) 1894–1903.
[34] I. Ochoa, J.A. Sanz-Herrera, J.M. Garcia-Aznar, M. Doblaré, D.M. Yunos, A.R. Boccaccini, Permeability evaluation of 45S5 Bioglass®-based scaffolds for bone tissue engineering, J. Biomech. 42 (2009) 257–260.
[35] D.D. Deligianni, N.D. Katsala, P.G. Koutsoukos, Y.F. Missirlis, Effect of surface roughness of hydroxyapatite on human bone marrow cell adhesion, proliferation, differentiation and detachment strength, Biomaterials 22 (1) (2001) 87–96.
[36] C.Y. Kim, A.E. Clark, L.L. Hench, Early stages of calcium-phosphate layer formation in bioglasses, J. Non-Cryst. Solids 113 (1989) 195–202.
[37] L.L. Hench, R.J. Splinter, W.C. Allen, T.K. Greenlee Jr., Bonding mechanisms at the interface of ceramic prosthetic materials, J. Biomed. Mater. Res. 2 (1) (1971) 117–141.
[38] W.Q. Yan, T. Nakamura, M. Kobayashi, H.M. Kim, F. Miyaji, T. Kokubo, Bonding of chemically treated titanium implants to bone, J. Biomed. Mater. Res. 37 (2) (1997) 267–275.
[39] T. Kokubo, F. Miyaji, H.M. Kim, T. Nakamura, Spontaneous formation of bonelike apatite layer on chemically treated titanium metals, J. Am. Ceram. Soc. 79 (1996) 1127–1129.
[40] H. Liu, H. Yazici, C. Ergun, T.J. Webster, H. Bermek, An in vitro evaluation of the Ca/P ratio for the cytocompatibility of nano-to-micron particulate calcium phosphates for bone regeneration, Acta Biomater. 4 (2008) 1472–1479.